Local Nonsimilarity Boundary-Layer Solutions

E. M. Sparrow,* H. Quack,† and C. J. Boerner‡
University of Minnesota, Minneapolis, Minn.

A new solution method for nonsimilarity boundary layers, applicable locally and independently of information from other streamwise positions, is described and implemented. The governing equations generated by the local nonsimilarity solution method are of the same type as those encountered in the treatment of similarity boundary layers. In addition to its local applicability, the utility of the new method is enhanced by its simplicity and directness, both in concept and in actual computations. Several nonsimilar velocity boundary-layer problems are solved herein with a view to illustrating the method, the participating nonsimilarities stemming from the freestream velocity distribution, surface mass transfer, and transverse curvature. On the basis of comparisons with available published information as well as of comparisons internal to the method itself, it may be concluded that the local nonsimilarity method provides results of high accuracy at all streamwise locations, except those near a point of separation.

Nomenclature

c_f = local friction coefficient, $2\tau_w/\rho U^2$
f = dimensionless stream function
G = χ-derivative of f
g = ξ-derivative of f
H = χ-derivative of G
h = ξ-derivative of g
L = reference length
R = cylinder radius
r = radial coordinate
Re_x = Reynolds number, Ux/ν
U = local freestream velocity
U_∞ = reference velocity; also, uniform freestream velocity
u = streamwise velocity component
v = transverse velocity component
v_w = velocity normal to surface
x = streamwise coordinate
y = transverse coordinate normal to surface
β = velocity parameter, Eq. (5)
η = transformed coordinate
ν = kinematic viscosity
ξ = transformed streamwise coordinate
ρ = density
τ_w = shear stress at wall
χ = transformed streamwise coordinate
ψ = stream function
Ω = velocity parameter, Eq. (30)

Introduction

MANY boundary-layer problems of contemporary interest do not admit similarity solutions. A number of solution methods involving different degrees of approximation and various levels of numerical effort have been proposed to deal with such problems. A review of nonsimilarity solution methods, along with citations of relevant publications, is available in a recent survey paper by Dewey and Gross.[1]

One frequently-used concept in the solution of nonsimilarity boundary layers is the principle of local similarity. In this approach, which will be illustrated later, the relevant boundary-layer equation (or equations), suitably transformed and divested of nonsimilar terms, is applied locally and independently at discrete streamwise locations. The transformed and simplified equation resembles that for a similarity boundary layer (i.e., it can be treated as an ordinary differential equation) and is solved by well established techniques. One of the particularly attractive features of the local similarity model is that the solution at a particular streamwise location can be found without having to perform calculations at upstream locations.

All nonsimilar boundary layers depart by varying degrees from the local similarity model. To evaluate small departures from local similarity, a series expansion about the locally-similar state has been proposed (e.g., Refs. 1–3).§ However, even the determination of the first term of the series appears to be a formidable undertaking.

In the present paper, a method for obtaining locally nonsimilar boundary-layer solutions is described and illustrated. The method preserves the most attractive aspects of the local similarity model (i.e., local solutions independent of upstream information; ordinary differential equations), but accounts for nonsimilarity of the boundary layer. Other attractive features of the new solution method are its simplicity and directness, both in concept and in application.

In illustrating the application of the new method, several boundary-layer velocity problems are solved. These include Howarth's retarded flow, cylinder in crossflow, flat plate with uniform surface mass transfer, and cylinder in longitudinal flow. The nonsimilarities encountered in these problems stem from three factors: 1) freestream velocity, 2) surface mass transfer, and 3) transverse curvature.

To provide perspective on the capabilities of the local nonsimilarity solution method, the wall shear results are compared with prior information from the published literature, particularly with accurate finite-difference and difference-differential solutions whenever available. In addition, velocity profiles are presented for those problems for which such information was heretofore unavailable.

Description of the Local Nonsimilarity Solution Method

Boundary-layer nonsimilarity may result from a variety of causes and, as was already noted, three classes of nonsimilarities are treated during the course of this investigation. However, in the initial exposition of the new solution method, it is thought best to deal with only one class of nonsimilarity. Therefore, in this section of the paper, attention is directed to boundary layers whose nonsimilarity is caused by spatial variations in the freestream velocity, such nonsimilarities

Received June 9, 1969; revision received January 23, 1970.
* Professor of Mechanical Engineering.
† Doctoral Candidate, ETH, Zurich, Switzerland.
‡ Doctoral Candidate.

§ Interested readers may wish to note that terms retained in Ref. 1 owing to $\epsilon'(\beta)$ are omitted in Ref. 3.

being, perhaps, the most common of all. In later sections, nonsimilarities caused by surface mass transfer and transverse curvature will be dealt with.

Consideration is given here to two-dimensional, constant property flows. However, the solution method can be extended without difficulty to accommodate more complex flows (for example, Mangler-type rotationally symmetric flows; variable property flows with coupled conservation equations).

The boundary layers to be studied in this section of the paper are, then, described by

$$u(\partial u/\partial x) + v(\partial u/\partial y) = U(dU/dx) + \nu(\partial^2 u/\partial y^2) \quad (1)$$

$$u = v = 0 \quad \text{at } y = 0, \quad u \to U(x) \text{ as } y \to \infty \quad (2)$$

where x and y denote the streamwise and transverse coordinates, respectively measured along and normal to the surface. $U(x)$ is the freestream velocity, which is a known function of x.

Transformation of the Boundary-Layer Equation

As a first step in the development of the solution method, the boundary layer is transformed from the x, y coordinate system to the ξ, η system, where ξ is related to x and η would be a similarity variable if the boundary layer were similar. The purpose of such a transformation is to lessen the dependence of the solution on the streamwise coordinate. There are any number of transformations that can be used. In computational experiments performed during the course of this investigation, a transformation, appearing in publications by Gortler[4] and Meksyn,[5] was found to be highly effective and is, therefore, employed here.¶

One defines

$$\xi = \int_0^x [U(x)/U_\infty](dx/L), \quad \eta = yU(x)/(2\nu L U_\infty \xi)^{1/2} \quad (3)$$

in which L is a reference length and U_∞ is a reference velocity that is taken as the velocity of the oncoming flow. In addition, the stream function is represented as

$$\psi = (2\nu L U_\infty \xi)^{1/2} f(\xi,\eta) \quad (4)$$

with a parameter β which depends on x (or ξ)

$$\beta = \left(\frac{2}{U^2}\right)\left(\frac{dU}{dx}\right)\int_0^x U dx \quad (5)$$

The outcome of the transformation is that the boundary-layer momentum equation (1) becomes

$$f''' + ff'' + \beta(1 - f'^2) = 2\xi[f'(\partial f'/\partial\xi) - f''(\partial f/\partial\xi)] \quad (6)$$

with boundary conditions

$$f(\xi,0) = f'(\xi,0) = 0, f'(\xi,\infty) = 1 \quad (7)$$

where the primes denote partial derivatives with respect to η. It may be observed that the momentum equation remains a partial differential equation after transformation, with the $\partial/\partial\xi$ terms on the right-hand side providing the major obstacle to solution.

Local Similarity

Before proceeding with the local nonsimilarity solution method, it is useful to examine Eq. (6) from the standpoint of the local similarity model. According to this approach, the right-hand side of Eq. (6) is postulated to be sufficiently small so that it may be approximated by zero, with the result that

$$f''' + ff'' + \beta(1 - f'^2) = 0 \quad (8)$$

subject to the boundary conditions in Eq. (7). The quantity β may be regarded as a known constant parameter at any streamwise location x(or ξ), so that Eq. (8), with the boundary conditions in Eq. (7), can be treated as an ordinary differential equation and solved by techniques appropriate to similarity boundary layers.

Turning to the rationale of the local similarity model, the reduction of Eq. (6) to (8) is clearly justifiable for values of ξ that are very close to zero. On the other hand, when ξ is not small, local similarity is based on the postulate that derivatives involving $\partial/\partial\xi$ are very small.

Local Nonsimilarity Solution Method

With the foregoing as background, a local solution method for nonsimilar boundary layers can now be developed. First, let

$$g(\xi,\eta) = \partial f/\partial\xi \quad (9)$$

so that the momentum equation (6) and its boundary conditions (7) become

$$f''' + ff'' + \beta(1 - f'^2) = 2\xi(f'g' - f''g) \quad (10)$$

$$f(\xi,0) = f'(\xi,0) = 0, f'(\xi,\infty) = 1 \quad (11)$$

Next, Eqs. (10) and (11) are differentiated with respect to ξ, with the result that

$$g''' + fg'' - 2\beta f'g' + f''g + (d\beta/d\xi)(1 - f'^2) = 2(f'g' - f''g) + 2\xi(\partial/\partial\xi)(f'g' - f''g) \quad (12)$$

$$g(\xi,0) = g'(\xi,0) = 0, g'(\xi,\infty) = 0 \quad (13)$$

The f and g functions appear in both Eqs. (10) and (12). If not for the presence of the term $\xi(\partial/\partial\xi)(f'g' - f''g)$, these equations could be treated as ordinary differential equations and solved locally. To provide the desired local autonomy for Eqs. (10) and (12), it is now assumed that the term $\xi(\partial/\partial\xi)(f'g' - f''g)$ can be dropped from Eq. (12). This reduction is readily justifiable for ξ values that are very close to zero, whereas when ξ is not small, one invokes the postulate that $(\partial/\partial\xi)(f'g' - f''g)$ is small.

The rationale for the aforementioned reduction is similar to that employed in deriving the local similarity model, but with a fundamental difference in the outcome. In the case of local similarity, it was postulated that for ξ values that are not near zero, $f'g' - f''g$ is sufficiently small so that the right-hand side of Eq. (6) can be approximated by zero. Similarly, in reducing Eq. (12), it was assumed that $(\partial/\partial\xi)(f'g' - f''g)$ is small for ξ values away from zero.

In the case of the local similarity model, the outcome is that a part of the momentum equation itself is lost. On the other hand, for the local non-similarity approach, the approximation is introduced in a subsidiary equation, that is, in Eq. (12), so that the momentum Eq. (10) remains intact and the nonsimilarity terms appearing therein are retained. It is thus expected that the local nonsimilarity approach should yield more accurate results for the wall shear and the velocity field than those of the local similarity model.

The governing equations for the local nonsimilarity model may now be brought together as

$$f''' + ff'' + \beta(1 - f'^2) = 2\xi(f'g' - f''g) \quad (14)$$

$$g''' + fg'' - 2\beta f'g' + f''g + (d\beta/d\xi)(1 - f'^2) = 2(f'g' - f''g) \quad (15)$$

$$f(\xi,0) = f'(\xi,0) = g(\xi,0) = g'(\xi,0) = g'(\xi,\infty) = 0, \quad f'(\xi,\infty) = 1 \quad (16)$$

For a given freestream flow, β and $d\beta/d\xi$ would be known at any streamwise position x(or ξ). Therefore, at a fixed streamwise position, β, $d\beta/d\xi$, and ξ may be regarded as known constants, and Eqs. (14) and (15) can be treated as a pair of simultaneous ordinary differential equations. The

¶ In response to a question by one of the referees, it is the opinion of the authors that the present solution method bears no special relation to the series method of Gortler.

solution of such equations is straightforward by techniques regularly employed for similarity boundary layers, about which brief comments will be made later.

Equations (14) and (15) will be referred to as the two-equation local nonsimilarity model. It represents the first stage in a succession of locally applicable multiequation systems which are expected to provide increasingly accurate results. The three-equation model will now be developed.

One begins by letting

$$h = \partial g/\partial\xi = \partial^2 f/\partial\xi^2 \tag{17}$$

so that the last term of Eq. (12) is

$$(\partial/\partial\xi)(f'g' - f''g) = g'^2 - gg'' + f'h' - f''h \tag{18}$$

Then, Eq. (12), with Eq. (18) incorporated, is differentiated with respect to ξ, yielding

$$h''' + fh'' - 2\beta(g'^2 + f'h') + f''h + 2gg'' - 4(d\beta/d\xi)f'g' + (d^2\beta/d\xi^2)(1 - f'^2) = 4(g'^2 - gg'' + f'h' - f''h) + 2\xi(\partial^2/\partial\xi^2) \times (f'g' - f''g) \tag{19}$$

To make the system consisting of Eqs. (10, 12, and 19) locally autonomous, one drops the term $\xi(\partial^2/\partial\xi^2)(f'g' - f''g)$ that appears on the right-hand side of Eq. (19). On the other hand, all terms in the momentum Eq. (10) and in the first subsidiary Eq. (12) are retained. One expects that since the approximation is made in an equation that is secondarily subsidiary to the momentum equation, the wall shear and velocity results from the three-equation model should be even more accurate than those of the two-equation model.

For convenience in later applications, the mathematical system representing the three-equation model may be brought together as

$$f''' + ff'' + \beta(1 - f'^2) = 2\xi(f'g' - f''g) \tag{20}$$

$$g''' + fg'' - 2\beta f'g' + f''g + (d\beta/d\xi)(1 - f'^2) = 2(f'g' - f''g) + 2\xi(g'^2 - gg'' + f'h' - f''h) \tag{21}$$

$$h''' + fh'' - 2\beta(g'^2 + f'h') + f''h + 2gg'' - 4(d\beta/d\xi)f'g' + (d^2\beta/d\xi^2)(1 - f'^2) = 4(g'^2 - gg'' + f'h' - f''h) \tag{22}$$

with boundary conditions on f, g, and h

$$f(\xi,0) = f'(\xi,0) = g(\xi,0) = g'(\xi,0) = h(\xi,0) = h'(\xi,0) = g'(\xi,\infty) = h'(\xi,\infty) = 0, f'(\xi,\infty) = 1 \tag{23}$$

Eqs. (20–22) may be treated as a set of coupled ordinary differential equations at any fixed value of ξ and solved by techniques appropriate to similarity boundary layers.

In taking a retrospective view of the just-developed local nonsimilarity solution method, it should be emphasized that it is primarily the solution for the f function and its derivatives that is relevant. For instance, the velocity field and wall shear are given by

$$u = Uf'(\xi,\eta) \tag{24}$$

$$\tau_w = [\mu U^2/(2\nu L U_\infty \xi)^{1/2}]f''(\xi,0) \tag{25}$$

The g and h functions are subsidiary and are, at best, of marginal interest.

Before concluding the general description of the solution method, it is appropriate to inquire whether the method provides, within itself, a way of assessing the accuracy of the results obtained therefrom. It is believed that such an assessment is obtainable by comparing the results provided by the successive equation systems (i.e., local similarity, the two-equation model, the three-equation model, etc.). For instance, if the results obtained from the two- equation model are essentially identical to those from the three-equation model, then high accuracy is believed to exist. That this is indeed the case will be demonstrated when specific problems are solved and discussed.

The just-described solution method will be applied to several boundary-layer velocity problems, the nonsimilarities of which stem from surface mass transfer and transverse curvature as well as from the freestream flow. As will be demonstrated later, the treatment of the former classes of nonsimilarity follows the same pattern as that already described for the latter.

Solution of the Ordinary Differential Equations

The procedure employed herein to solve the ordinary differential equations of the local nonsimilarity model closely resembles that outlined by Dewey and Gross,[1] with some differences in detail. In particular, it was found advantageous to start the computations for a particular case with a relatively small value of η_{max} (η_{max} is the numerical approximation to $\eta = \infty$), and then to successively increase η_{max} until the preassigned tolerances on the values of dependent variables at η_{max} are satisfied. The computations were terminated when $|f' - 1|$, g',h',f'',g'', and h'' were on the order of $10^{-6} - 10^{-7}$ at η_{max}.

Interested readers may wish to consult papers by Nachtsheim and Swigert[6] and by Hayday and co-workers[7] for further background on the solution of ordinary differential equations relevant to boundary layers.

Howarth's Retarded Flow

One of the best-known boundary-layer flows which is nonsimilar as a result of spatial variations in the freestream velocity is Howarth's retarded flow, for which

$$U(x)/U_\infty = 1 - (x/L) \tag{26}$$

This problem affords an attractive opportunity for testing the local nonsimilarity solution method, inasmuch as accurate difference-differential[8] and finite-difference[9] solutions are available and, furthermore, the local similarity results are substantially in error.

The formulation of the preceding section is directly applicable to the problem at hand, and some computer solutions were performed using the equations derived therein. However, for historical reasons only, the full set of solutions to the problem was carried out employing an alternate group of equations, the derivation of which begins by applying the transformation**

$$\xi = x/L,\ \eta = y(U/\nu x)^{1/2},\ \psi = (\nu U x)^{1/2} f(\xi,\eta) \tag{27}$$

to the boundary-layer momentum equation (1), with the result

$$f''' + [(\Omega + 1)/2]ff'' + \Omega(1 - f'^2) = \xi(f'g' - f''g) \tag{28}$$

with boundary conditions

$$f(\xi,0) = f'(\xi,0) = 0, f'(\xi,\infty) = 1 \tag{29}$$

The g function is defined by Eq. (9) and

$$\Omega = (x/U)(dU/dx) = (x/L)/[(x/L) - 1] \tag{30}$$

Using Eq. (28) as a basis, the derivation of the two- and three-equation local nonsimilarity models proceeds exactly as before, and there is no need for further elaboration here.

Prime consideration will be given to the wall shear τ_w, which may be expressed in terms of the usual dimensionless groups and of the $f''(\xi,0)$ from the solutions of the governing

** This is the transformation used by Smith and Clutter[8] as a prelude to their difference-differential solutions of the problem.

equations as

$$c_f(Re_x)^{1/2} = 2f''(\xi,0) \tag{31}$$

where

$$c_f = 2\tau_w/\rho U^2,\ Re_x = Ux/\nu \tag{32}$$

The $c_f(Re_x)^{1/2}$ results from the local nonsimilarity solutions are presented in Fig. 1, where they are compared with corresponding results from difference-differential and finite-difference solutions (which are essentially identical in the x/L range of the figure) and from the local similarity model. Inspection of the figure reveals that the results from the local similarity, two-equation, and three-equation models are arranged in a heirarchy of increasing accuracy, relative to the difference-differential and finite-difference results as a standard. The local similarity model (which is, in essence, a one-equation model) is seriously in error. The two-equation model somewhat over-corrects the local similarity model and provides results of significantly greater accuracy. In turn, the three-equation model slightly over-corrects the two-equation model and furnishes even more accurate results. Furthermore, the successive levels of the local nonsimilarity model bracket the exact solution. It will be found that the just-described pattern will be reproduced in other boundary-layer problems studied herein.

Further study of the figure shows that when the results of the two- and three-equation models are in substantial agreement, then the results are of high accuracy. This characteristic furnishes a means of estimating the level of accuracy of the results provided by the local nonsimilarity method.

The good accuracy of the results from the three-equation model provides a highly affirmative impression of the local nonsimilarity method. The deviations that appear at the larger x/L are due to the imminence of separation ($x/L \sim 0.12$). It is not expected nor intended that the method will be applicable in the very near neighborhood of separation. However, on the basis of Fig. 1 and of the findings of subsequent sections, it is expected that away from the separation point, the new solution method will yield results of acceptable accuracy.

In response to a request by one of the referees, the results given by a three-term Gortler series have also been included in Fig. 1. It is seen that the accuracy of the results provided by this series is not quite as good as that provided by the three-equation model.

Cylinder in Crossflow

Another well-known boundary-layer flow whose nonsimilarity is due to the freestream velocity distribution is the cylinder in crossflow. Consideration is given here to the case of irrotational potential flow in the freestream, so that

$$U(x)/U_\infty = 2\sin(x/R) \tag{33}$$

in which U_∞ is the velocity of the oncoming flow, R is the cylinder radius, and x is the circumferential distance measured from the forward stagnation point.

Local nonsimilarity solutions for this problem were obtained by specializing the general formulation that was presented earlier in the paper. In particular, corresponding to the $U(x)$ of Eq. (33), the ξ, η, and β of Eqs. (3) and (5) become

$$\xi = 2[1 - \cos(x/R)],\ \eta = (y/R)(U_\infty R/\nu)^{1/2}\sin(x/R)/[1 - \cos(x/R)]^{1/2} \tag{34}$$

$$\beta = [2\cos(x/R)]/[1 + \cos(x/R)] \tag{35}$$

The equations which were employed in carrying out the solutions were as follows: 1) local similarity, Eq. (10) with right side deleted; 2) two-equation model, Eqs. (14) and (15); 3) three-equation model, Eqs. (20–22).

Once again, primary attention is focussed on the wall shear τ_w, the dimensionless representation of which takes the form

$$c_f(UR/\nu)^{1/2}[1 - \cos(x/R)]^{1/2}/[2\sin(x/R)]^{1/2} = f''(\xi,0) \tag{36}$$

where c_f is defined in Eq. (32) and the $f''(\xi,0)$ are from the solutions of the aforementioned governing equations.

The dimensionless wall shear results from the local similarity and nonsimilarity solutions are presented in Fig. 2. Also shown in the figure is a curve corresponding to difference-differential[10] and finite-difference[9] solutions, which will be taken as a standard against which the other curves are to be compared; these results are essentially identical in the x/R range of the figure. Inspection of the figure reveals trends that are qualitatively identical to those already discussed in connection with Fig. 1. That is, increasingly more accurate results are obtained as one passes from the local similarity model to the two-equation model and thence to the three-equation model. Furthermore, the successive curves from these models bracket the exact solution.

The results from the three-equation model are seen to be virtually exact up to $x/R = 1.4$, which corresponds to an angular position approximately 80° from the forward stagnation point. For larger values of x/R, the effects of the downstream separation become increasingly more important and greater deviations are evident in the c_f results.

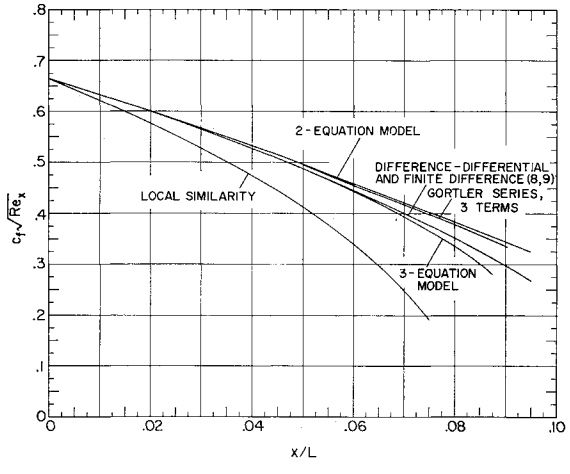

Fig. 1 Wall shear results, Howarth's retarded flow.

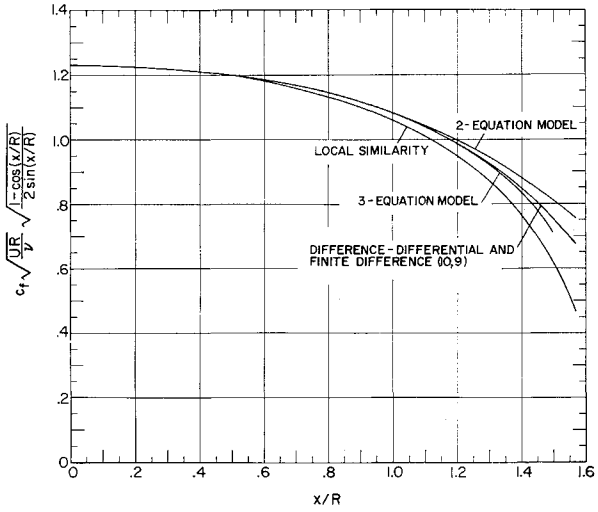

Fig. 2 Wall shear results, cylinder in crossflow.

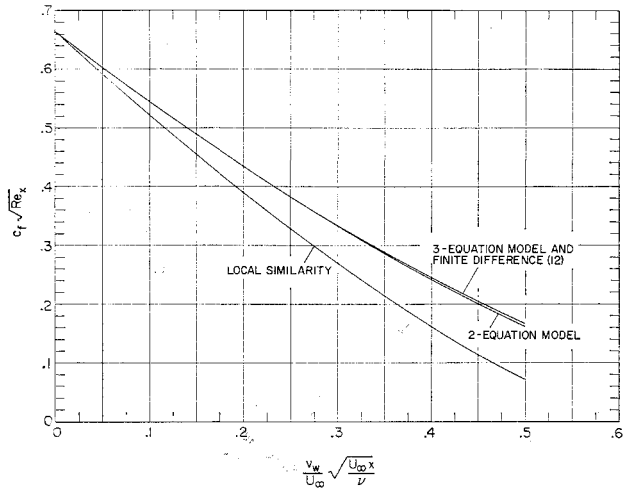

Fig. 3 Wall shear results, flat plate with uniform blowing at the surface.

It is believed that findings presented in Fig. 2 are highly favorable to the local nonsimilarity solution method.

Flat Plate with Uniform Surface Mass Transfer

It is well known that for the flat plate with surface mass transfer, similarity boundary-layer solutions are possible only if $v_w \sim x^{-1/2}$, where $v_w = v(x,0)$ and x is the streamwise coordinate measured from the leading edge. Therefore, the case of uniform surface mass transfer gives rise to a nonsimilarity boundary layer. Furthermore, the errors incurred by employing the local similarity model are markedly greater for uniform mass injection (blowing) than for uniform suction.[11]

This section of the paper is, then, concerned with the application of the local nonsimilarity solution method to the flat plate with uniform blowing. This problem differs from those treated in the prior sections in that the nonsimilarity is now introduced through the boundary conditions at the surface. Consequently, in the discussion that follows, primary emphasis will be given to detailing how the new solution method accommodates such nonsimilarities.

The starting point of the analysis is the application of Gortler's transformation, Eqs. (3–5), to the boundary-layer momentum Eq. (1). Upon noting that $\beta = 0$ since $U(x) = U_\infty = \text{const}$, the transformed momentum Eq. (6) becomes

$$f''' + ff'' = 2\xi[f'(\partial f'/\partial\xi) - f''(\partial f/\partial\xi)] \tag{37}$$

where

$$\eta = y(U_\infty/2\nu x)^{1/2},\ \xi = x/L \tag{38}$$

The boundary conditions that $v = v_w$ and $u = 0$ at $y = 0$ and that $u \to U_\infty$ as $y \to \infty$ transform to

$$f + 2\xi(\partial f/\partial\xi) = -(v_w/U_\infty)(2xU_\infty/\nu)^{1/2} \text{ at } \eta = 0 \tag{39}$$

$$f'(\xi,0) = 0, f'(\xi,\infty) = 1 \tag{40}$$

The novel aspect of the problem is the boundary condition (39).

To proceed, one introduces a further change of variables defined by

$$\chi = (v_w/U_\infty)(2xU_\infty/\nu)^{1/2} = (2\xi)^{1/2} \text{ and } G = \partial f/\partial\chi \tag{41}$$

with the result that

$$f''' + ff'' = \chi(f'G' - f''G) \tag{42}$$

$$f + \chi = -\chi G \text{ at } \eta = 0 \tag{43}$$

$$f'(\chi,0) = 0, f'(\chi,\infty) = 1 \tag{44}$$

Equations (42–44) serve as the basis for the local similarity and local nonsimilarity solution methods. The local similarity model follows by replacing the right-hand sides of Eqs. (42) and (43) by zero. To derive the two-equation local nonsimilarity model, one begins by differentiating Eq. (42) with respect to χ and replaces $\partial f/\partial\chi$, $\partial f'/\partial\chi$, ... by G,G', ..., whereafter the term involving $\chi(\partial/\partial\chi)(f'G' - f''G)$ is deleted. The resulting differential equation is to be solved simultaneously with Eq. (42).

The boundary conditions for the two-equation model are derived by differentiating Eqs. (43) and (44) with respect to χ. From the first of these, there follows

$$G + 1 = -G - \chi(\partial G/\partial\chi) \text{ at } \eta = 0 \tag{45}$$

Upon deleting the term involving $\partial G/\partial\chi$, Eq. (45) yields $G(\chi,0) = -\frac{1}{2}$ and, in turn, $f(\chi,0) = -(\frac{1}{2})\chi$ from Eq. (43). The other boundary conditions follow directly, so that

$$f(\chi,0) = -(\tfrac{1}{2})\chi, f'(\chi,0) = 0, f'(\chi,\infty) = 1 \tag{46}$$

$$G(\chi,0) = -\tfrac{1}{2}, G'(\chi,0) = 0, G'(\chi,\infty) = 0 \tag{47}$$

For the three-equation model, one generates G''' and H''' equations ($G = \partial f/\partial\chi, H = \partial G/\partial\chi$) by successive differentiations of Eq. (42) with respect to χ and deletes the term involving $\chi(\partial^2/\partial\chi^2)(f'G' - f''G)$. For the boundary conditions, double differentiation of Eq. (43) with respect to χ yields

$$2H = -H - \chi(\partial H/\partial\chi) \text{ at } \eta = 0 \tag{48}$$

whereupon, after deleting $\partial H/\partial\chi$, it follows that $H(\chi,0) = 0$, and from Eqs. (45) and (43), $G(\chi,0) = -\frac{1}{2}$ and $f(\chi,0) = -(\frac{1}{2})\chi$, respectively. The other boundary conditions are derived by single and double differentiations of Eq. (44). Thus, the boundary conditions for the three-equation model are

$$f(\chi,0) = -(\tfrac{1}{2})\chi, f'(\chi,0) = 0, f'(\chi,\infty) = 1 \tag{49}$$

$$G(\chi,0) = -\tfrac{1}{2}, G'(\chi,0) = 0, G'(\chi,\infty) = 0 \tag{50}$$

$$H(\chi,0) = 0, H'(\chi,0) = 0, H'(\chi,\infty) = 0 \tag{51}$$

With the derivation of the governing equations and boundary conditions now complete, attention may be turned to the presentation of the results. The local wall shear stress is expressible as

$$c_f(Re_x)^{1/2} = 2^{1/2}f''(\chi,0) \tag{52}$$

$$c_f = 2\tau_w/\rho U_\infty^2,\ Re_x = U_\infty x/\nu \tag{53}$$

Figure 3 shows curves for $c_f(Re_x)^{1/2}$ as a function of the dimensionless streamwise coordinate $(v_w/U_\infty)(U_\infty x/\nu)^{1/2}$. Re-

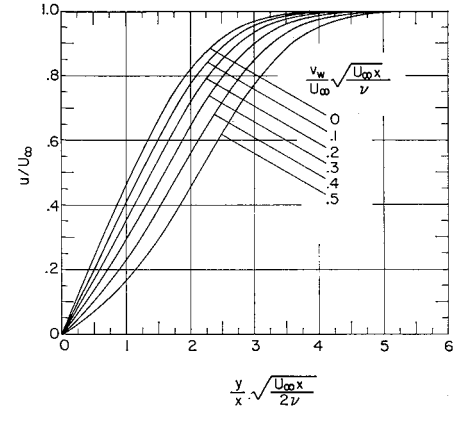

Fig. 4 Representative velocity profiles, flat plate with uniform blowing at the surface.

sults are given for local similarity, the two-equation model, the three-equation model, and a finite-difference solution.[12]

Within the scale of the figure, the results for the three-equation model are indistinguishable from the presumably exact results of the finite-difference solution. Furthermore, the results provided by the two-equation model are also of very high accuracy. This clear success of the local nonsimilarity solution method is further accentuated when account is taken of the significant errors in the results of the local similarity model [e.g., the $c_f(Re_x)^{1/2}$ at an abscissa of 0.5 is 43% of the exact value].

The findings of Fig. 3 lend strong support to the utility of the new solution method. The information presented in the figure also affirms the characteristic that when the results of the two- and three-equation models are in close agreement, they are of high accuracy.

Boundary-layer velocity profiles for the flat plate with uniform surface blowing are apparently unavailable in the literature, except in the neighborhood of the separation point.[12] Velocity profiles are provided directly by the present solutions in the form $u/U_\infty = f'$, a presentation of which is made in Fig. 4 as a function of $(y/x)(U_\infty x/2\nu)^{1/2}$ for parametric values of $(v_w/U_\infty)(U_\infty x/\nu)^{1/2}$. The successive profiles are increasingly S-shaped. This trend is in qualitative agreement with that for the velocity profiles corresponding to similarity blowing (i.e., $v_w \sim x^{-1/2}$).

Cylinder in Longitudinal Flow

For boundary-layer flow longitudinal to a cylinder, the transverse curvature of the surface gives rise to a nonsimilar velocity field. The nonsimilarity is encountered directly in the governing equations, in contrast to nonsimilarities caused by surface or freestream boundary conditions. In further contrast to the boundary-layer problems treated in the earlier sections, the flow now under consideration does not have a separation point.

The conservation equations relevant to the problem, written in x,r cylindrical coordinates, are

$$u(\partial u/\partial x) + v(\partial u/\partial r) = (\nu/r)(\partial/\partial r)[r(\partial u/\partial r)] \quad (54)$$

$$(\partial/\partial x)(ru) + (\partial/\partial r)(rv) = 0 \quad (55)$$

By applying a transformation first suggested by Seban and Bond,[13] i.e.,

$$\xi = (4/R)(\nu x/U_\infty)^{1/2},\ \eta = (U_\infty/\nu x)^{1/2}(r^2 - R^2)/4R \quad (56)$$

$$\psi = R(\nu U_\infty x)^{1/2} f(\xi,\eta)$$

the momentum Eq. (54) becomes

$$(1 + \eta\xi)f''' + ff'' + \xi f' = \xi(f'g' - f''g) \quad (57)$$

in which $g = \partial f/\partial\xi$ as before. In terms of the transformed variables, the boundary conditions are

$$f(\xi,0) = f'(\xi,0) = 0,\ f'(\xi,\infty) = 2 \quad (58)$$

In the foregoing, R denotes the radius of the cylinder and $U(x) = U_\infty$ = constant is the freestream velocity. The boundary condition $f(\xi,0) = 0$ corresponds to an impermeable surface (i.e., $v_w = 0$). The ξ coordinate can be taken as a measure of the boundary-layer thickness relative to the cylinder radius.

To derive the local similarity model, one replaces the right-hand side of Eq. (57) by zero. To generate the two-equation model, Eq. (57) is differentiated with respect to ξ, the term involving $\xi(\partial/\partial\xi)(f'g' - f''g)$ is deleted, and $\partial f/\partial\xi$, $\partial f'/\partial\xi$, ... are replaced by g,g', ... The thus derived g''' equation, taken together with Eq. (57) and with appropriate boundary conditions for f and g, constitutes the two-equation model. The three-equation model is constructed by two successive ξ differentiations of Eq. (57), and so on and so forth as in the earlier problems. The derivation

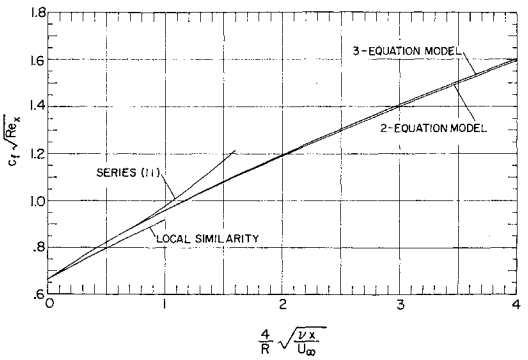

Fig. 5 Wall shear results, cylinder in longitudinal flow, range of small and intermediate x.

of the boundary conditions is straightforward, the end result being given by Eqs. (23), except that now, $f'(\xi,\infty) = 2$.

Turning now to the numerical results, consideration may first be given to the local wall shear expressed as the $c_f(Re_x)^{1/2}$ grouping, where

$$c_f(Re_x)^{1/2} = (\tfrac{1}{2})f''(\xi,0) \quad (59)$$

and c_f and Re_x are defined in Eq. (53). The presentation of the $c_f(Re_x)^{1/2}$ results is made in two figures, respectively for smaller ξ and for larger ξ. The first of these figures, Fig. 5, covers the range $0 \leq \xi \leq 4$. Curves are shown for the $c_f(Re_x)^{1/2}$ results from local similarity and from the two- and three-equation models.

Also appearing in the figure is a curve based on a series solution of Eq. (57) about $\xi = 0$. The series solution was originally devised by Seban and Bond,[13] who evaluated the first three terms. Numerical corrections were subsequently made by Kelly.[14] More recently, Wanous and Sparrow[11] further refined the existing numerical information and, in addition, provided a fourth term of the series.

Within the knowledge of the authors, neither difference-differential nor finite-difference solutions of the problem have been reported in the published literature.

From an inspection of Fig. 5, it is seen that the results from the two- and three-equation models are in excellent agreement over the entire range of ξ considered therein. The greatest deviations between the two curves is about 0.5 %. Consequently, there is every reason to believe the $c_f(Re_x)^{1/2}$ results represented by these curves are of high accuracy. The results from the series solution appear to be valid in the range between $\xi = 0$ and $\xi = 1$, whereafter increasingly larger errors are incurred. The local similarity solutions were terminated at $\xi = 1$, at which point the $c_f(Re_x)^{1/2}$ value is about 4.4% less than that of the two- and three-equation models.

The range of very large x (i.e., very large ξ) was previously investigated by Glauert and Lighthill[15] by a series expansion about $x = \infty$, three terms of the series having been evaluated. These authors suggested that the shear stress results given by their solution are applicable for $\nu x/U_\infty R^2 > 100$†† (i.e., $\xi > 40$). In addition, Glauert and Lighthill constructed an interpolation curve for the wall shear to bridge the gap between the small x series of Seban, Bond, and Kelly and their own large x series.

The results of the present analysis are compared with those of Glauert and Lighthill in Fig. 6, the coordinates of the figure being those of the just-named authors. In terms of the variables of the present analysis, the ordinate and abscissa groupings may be written as

$$2\pi R\tau_w/\mu U_\infty = 2\pi f''(\xi,0)/\xi,\ \nu x/U_\infty R^2 = (\xi/4)^2 \quad (60)$$

†† At $\nu x/U_\infty R^2 = 100$, the third term of the series is 9% of the first two.

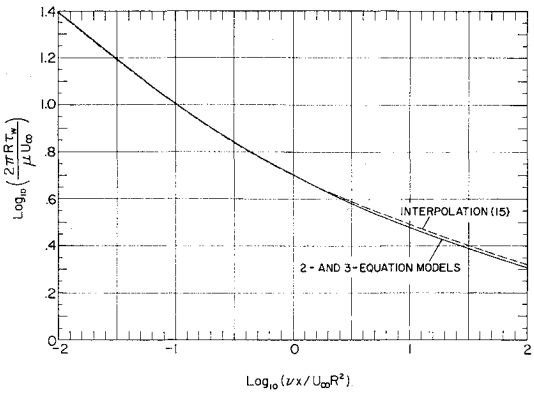

Fig. 6 Wall shear results, cylinder in longitudinal flow, range of intermediate and large x.

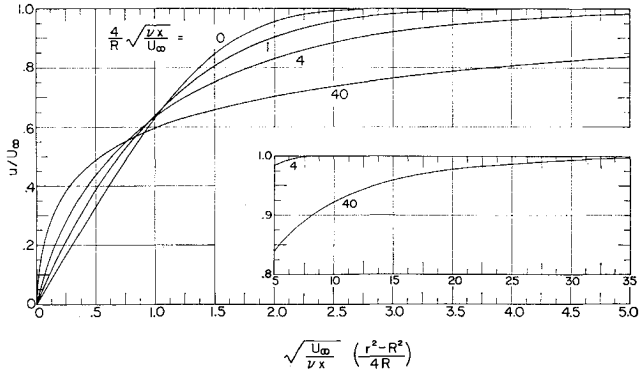

Fig. 7 Representative velocity profiles, cylinder in longitudinal flow.

The range of the abscissa variable corresponds to a range of ξ from 0.4 to 40.

Within the scale of the figure, the results from the two- and three-equation models are essentially coincident and are, therefore, plotted as a single curve (solid line). This can be taken as an affirmation of the high accuracy of these results. The dashed line represents the interpolation curve of Glauert and Lighthill. The agreement between the solid and dashed lines is highly satisfactory over the entire abscissa range of the figure. Indeed, in view of Glauert and Lighthill's estimate that their results may be in error by one in the second significant figure, the level of agreement indicated in Fig. 6 is as good as could be attained even if the present results were exact.

Figure 6 may be appraised as providing further support for the utility of the local nonsimilarity solution method.

Inasmuch as velocity profiles for the present problem do not appear to be available in the published literature, a presentation of such information is made in Fig. 7. In the figure, u/U_∞ is plotted as a function of $(U_\infty/\nu x)^{1/2}(r^2 - R^2)/4R = \eta$ for parametric values of the dimensionless streamwise coordinate $(4/R)(\nu x/U_\infty)^{1/2}$. It is seen from the figure that the character of the velocity profiles changes markedly as one proceeds downstream along the cylinder. The most evident changes are the substantial growth in the boundary-layer thickness and the increase of $\partial(u/U_\infty)/\partial\eta$ at the wall.

Concluding Remarks

In this paper, a method for obtaining locally nonsimilar boundary-layer solutions has been described and implemented by application to several boundary-layer velocity problems. In addition to providing locally autonomous results, the utility of the new method is enhanced by its simplicity and directness, both in concept and in application. Among the several problems used to illustrate the method, nonsimilarities resulting from the freestream velocity distribution, surface mass transfer, and transverse curvature are treated.

In the presentation and appraisal of the numerical results, primary emphasis was placed on the local wall shear stress. On the basis of comparisons with available published information, as well as of comparisons internal to the method itself (that is, comparisons between the two- and three-equation models), it may be concluded that the local nonsimilarity solution method provides results of good accuracy at streamwise locations away from the separation point. Furthermore, the aforementioned internal comparisons serve as a means for estimating the accuracy of the results.

Owing to the expository nature of the paper, the formulation and applications presented herein have dealt only with constant-property velocity boundary layers. The treatment of more complex situations (e.g., variable property flows with coupled conservation equations) appears to be conceptually clear, but computational experiments dealing with such problems still remain to be carried out.

References

[1] Dewey, C. F., Jr. and Gross, J. F., "Exact Similar Solutions of the Laminar Boundary Layer Equations," *Advances in Heat Transfer*, Vol. 4, Academic Press, New York, 1967, pp. 317–446.

[2] Merk, H. J., "Rapid Calculations for Boundary-Layer Transfer Using Wedge Solutions and Asymptotic Expansions," *Journal of Fluid Mechanics*, Vol. 5, No. 3, April 1959, pp. 460–480.

[3] Evans, H. L., *Laminar Boundary-Layer Theory*, Addison-Wesley, Reading, Mass., 1968.

[4] Gortler, H., "A New Series for the Calculation of Steady Laminar Boundary Layer Flows," *Journal of Mathematics and Mechanics*, Vol. 6, No. 1, Jan. 1957, pp. 1–66.

[5] Meksyn, D., *New Methods in Laminar Boundary Layer Theory*, Pergamon Press, Oxford, 1961.

[6] Nachtsheim, P. R. and Swiger, P., "Satisfaction of Asymptotic Boundary Conditions in Numerical Solution of Systems of Nonlinear Equations of Boundary-Layer Type," TN D-3004, 1965, NASA.

[7] Hayday, A. A., Bowlus, D. A., and McGraw, R. A., "Free Convection from a Vertical Flat Plate With Step Discontinuities n Surface Temperature," *Journal of Heat Transfer*, Vol. C89, No. 3, Aug. 1967, pp. 244–250.

[8] Smith A. M. O. and Clutter, D. W., "Solutions of the Incompressible Laminar Boundary Layer Equations," *AIAA Journal*, Vol. 1, No. 9, Sept. 1963, pp. 2062–2071.

[9] Schönauer, W., "Ein Differenzenverfahren zur Lösung der Grenzschichtgleichung für stationäre, laminare, inkompressible Strömung," *Ingenieur Archiv*, Vol. 33, No. 3, Feb. 1964, pp. 173–189.

[10] Terrill, R. M., "Laminar Boundary Layer Flow Near Separation With and Without Suction," *Philosophical Transactions of the Royal Society of London, Ser. A*, Vol. 253, No. 1022, Sept. 1960, pp. 55–100.

[11] Wanous, D. J. and Sparrow, E. M., "Longitudinal Flow Over a Circular Cylinder With Surface Mass Transfer," *AIAA Journal*, Vol. 3, No. 1, Jan. 1965, pp. 147–149.

[12] Catherall, D., Stewartson, K., and Williams, P. G., "Viscous Flow Past a Flat Plate With Uniform Injection," *Proceedings of the Royal Society, Ser. A*, Vol. 284, No. 1398, March 1965, pp. 370–396.

[13] Seban, R. A. and Bond, R., "Skin Friction and Heat Transfer Characteristics of a Laminar Boundary Layer on a Cylinder in Axial Incompressible Flow," *Journal of the Aeronautical Sciences*, Vol. 18, No. 10, Oct. 1951, pp. 671–675.

[14] Kelly, H. R., "A Note on the Laminar Boundary Layer on a Cylinder in Axial Incompressible Flow," *Journal of the Aeronautical Sciences*, Vol. 21, No. 9, Sept. 1954, p. 634.

[15] Glauert, M. B. and Lighthill, M. J., "The Axisymmetric Boundary Layer on a Long Cylinder," *Proceedings of the Royal Society, Ser. A*, Vol. 230, No. 1181, June 1966, pp. 188–203.